

# The use of palladium nanoparticles supported on active carbon for synthesis of disproportionated rosin (DPR)

Ramin Mostafalu<sup>1</sup> · Akbar Heydari<sup>1</sup> · Abbas Banaei<sup>2</sup> · Fatemeh Ghorbani<sup>2</sup> · Marzban Arefi<sup>1</sup>

Received: 6 December 2016 / Accepted: 12 January 2017 / Published online: 28 January 2017  
© The Author(s) 2017. This article is published with open access at Springerlink.com

**Abstract** Disproportionated rosin (DPR) is a mixture of rosin acids with dehydro-abietic acid as its major component. Alkaline salts of DPR are used as emulsifier surfactant in emulsion polymerization reactions. In this work, synthesis of DPR by the use of palladium nanoparticles loaded on activated carbon was studied. The nanocatalyst was characterized by TEM, SEM, XRD, N<sub>2</sub> adsorption-desorption and AAS. The reusability of the prepared nanocatalyst was successfully examined three times with only a very slight loss of catalytic activity.

**Keywords** Disproportionated rosin · DPR · Gum rosin · Palladium nanoparticles · Palladium-carbon

## Introduction

Disproportionated rosin (DPR) is a mixture of rosin acids with dehydro-abietic acid (DAA) (**2a**) as its major component [1]. Because of its low brittleness, high thermal stability, good oxidation resistance and light color, DPR is widely used in the production of butadiene and chloroprene rubber [2]. Alkaline salts of DPR are used as emulsifier

surfactant in emulsion polymerization reactions. This reaction is used for polystyrene and styrene butadiene rubber (SBR) preparation in petrochemical industries [3, 4]. The main constituent of the DPR (i.e., DAA) is also of potential value in the pharmaceutical industry and a number of its derivatives have many biological activities such as anti-cancer effects [5–7].

Disproportionation of rosin is described as a hydrogen exchange between molecules of resin [8, 9]. The main product of the reaction is DAA, and reaction can be viewed as the conversion of abietic acid (AA) to DAA (Fig. 1). At temperatures between 250 and 280 °C, the reaction is very slow and the addition of a catalyst increases the reaction rate.

Iodide, sulfur, lithium and iron salt, have traditionally been used to promote or catalyze disproportionation of rosin [9–11]. At the present time, palladium catalysts have been of great interest, in part because of the good properties that the DPR feature regarding light color, low odor, medium softening-point, and excellent resistance to oxidation [1, 2, 12–15]. In the continuation of our research [16–21], the disproportionation of rosin with Pd nanoparticles supported on activated carbon (AC) was studied in this work.

## Experimental section

### Materials and methods

The reagents were purchased from the Merck, Sigma-Aldrich and Daejung companies and were used without further purification. The starting gum rosin was commercially available. For TEM studies, samples were placed on copper grids covered with carbon film and examined with a

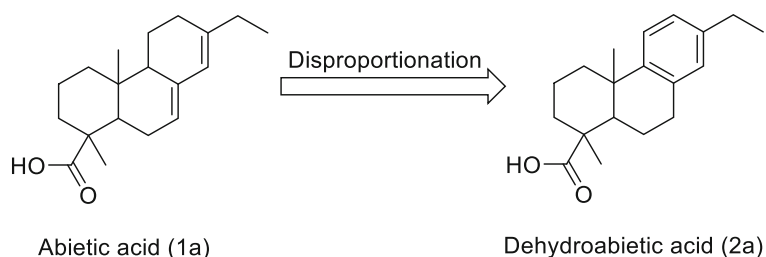
**Electronic supplementary material** The online version of this article (doi:10.1007/s40097-017-0220-y) contains supplementary material, which is available to authorized users.

✉ Akbar Heydari  
heydar\_a@modares.ac.ir

<sup>1</sup> Chemistry Department, Tarbiat Modares University, P.O. Box 14155-4838, Tehran, Iran

<sup>2</sup> Research and Development, Padideh Shimi Jam Co., Eshtehard Industrial Town, Karaj, Iran

**Fig. 1** Disproportionation of rosin



300 keV transmission electron microscope (TEM) JEM-3010 UHR (Jeol Ltd., Japan), equipped with a retractable high-resolution slow scan CCD-Camera (Gatan Inc., USA) with GOS phosphorous scintillator and lanthanum hexaboride cathode as the electron source. The X-ray powder patterns were recorded with a D8 ADVANCE (Bruker, Germany) diffractometer (CuK-radiation). Pd atomic absorption spectroscopy (AAS) was performed on an Atomic Absorption Spectrometer Varian SpectrAA 110. Prior to analysis, the sample was added to hydrochloric acid and  $\text{H}_2\text{O}_2$  and the reaction was carried out for 180 min at 90 °C. The solutions were then diluted, and analyzed by AAS.

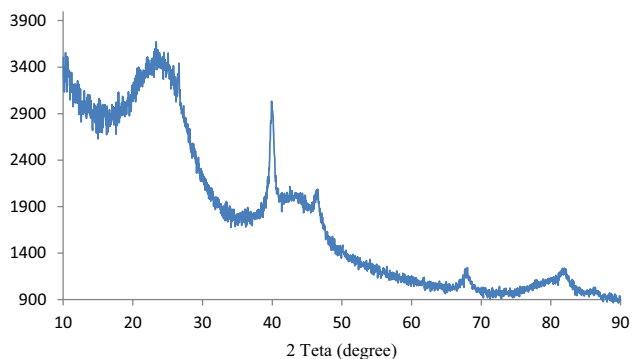


**Fig. 2** XRD pattern of Pd-NP-AC catalyst

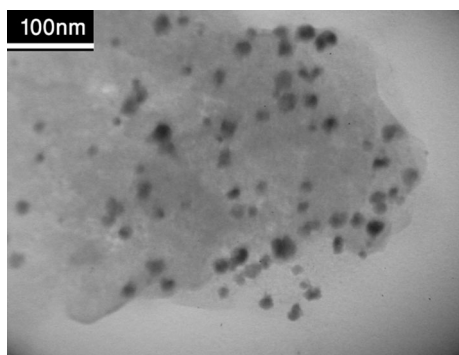


**Fig. 3** TEM image of Pd-NP-AC catalyst

### Preparation of palladium chloride

Palladium chloride is prepared by dissolving 1 g palladium metal in 4 ml freshly prepared aqua regia (mixture of nitric acid (99%) and hydrochloric acid (37%)) optimally in a volume ratio of (1:3) for 4 h at 80 °C. After 4 h a blood-red solution was obtained.

### Preparation of palladium nanoparticles loaded on activated carbon (Pd-NP-AC)

Pd nanoparticles were loaded on AC through a liquid phase reduction method. 19 g AC was suspended in 50 ml of water. Prepared palladium chloride was added and the reaction was continued for 2 h at 80 °C. Subsequently, the mixture was filtered in vacuum and rinsed using Millipore water. Prepared active carbon–palladium chloride was suspended in 60 ml of water. The pH of solution was adjusted to 9 by the use of NaOH and the suspension was stirred for 2 h. After 2 h, 60 ml of formalin (37%) reductant was added dropwise to the solution. The obtained suspension was magnetically stirred for two additional hours at 80 °C. Subsequently, the mixture was filtered in vacuum and rinsed using Millipore water. The resultant product was dried in a furnace at 105 °C overnight. The final amount of Pd loaded in sample was determined by atomic absorption.

### Disproportionation of rosin by Pd-NP-AC catalyst

100 g of rosin were inserted into a 250-ml three-neck round-bottom flask equipped with a mechanical stirrer, temperature sensor and condenser. The reaction was run at 280 °C in an  $\text{N}_2$  atmosphere to avoid oxidation. Once the reaction temperature was reached, the Pd-NP-AC catalyst (0.05% w/w) was added to the reaction. At the reaction temperature, a zero time sample was withdrawn before the catalyst was added, and more samples were taken during the first 6 h following the addition of the catalyst. A quantitative GC–FID analysis of the withdrawn samples was performed. Samples were methylated with tetramethylammonium hydroxide solution (10%) and analyzed on an Agilent model 7890A gas chromatograph with a flame



**Fig. 4** Elemental maps of the Pd-NP-AC catalyst with carbon on the left and palladium on the right

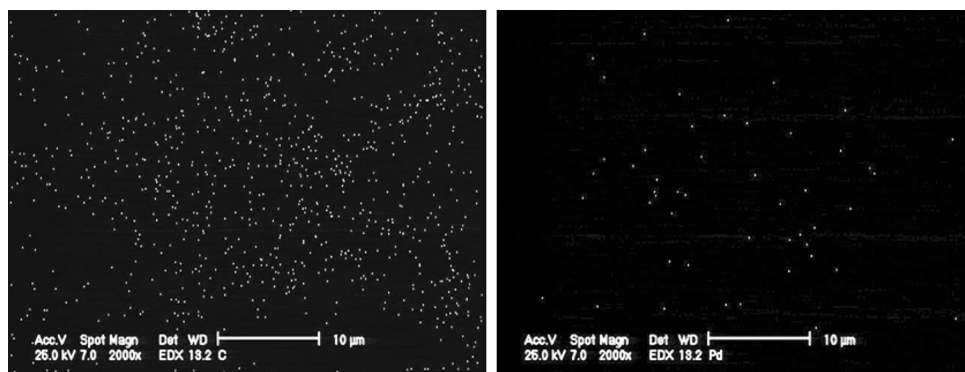


**Fig. 5** SEM images of the Pd-NP-AC catalyst

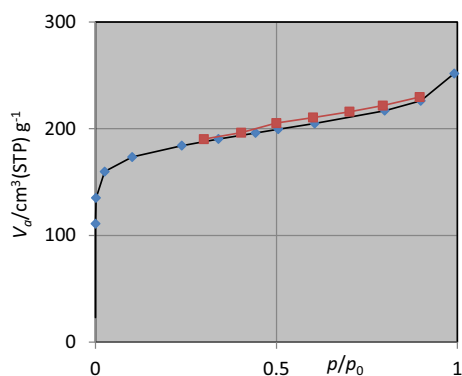
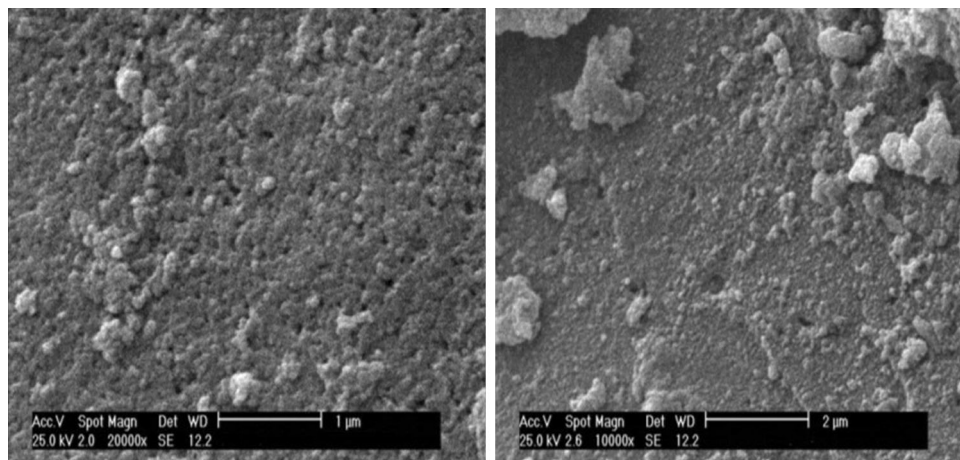
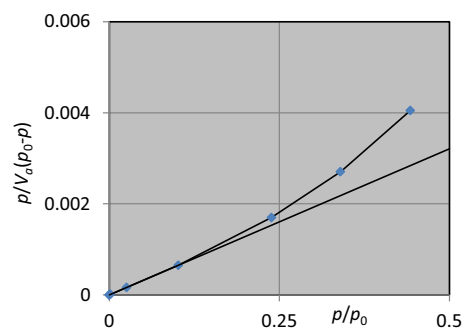


**Fig. 6** Adsorption/desorption isotherm of Pd-NP-AC catalyst

ionization detector. The instrument conditions are as follows:

Inlet: heater = 300 °C; pressure = 10.8 psi; total flow = 14 ml/min;  
 Septum purge: flow = 3 ml/min; split = 10:1;  
 Analytical column: DB 1701 (60 m);  
 Oven: initial = 100 °C, 5 min; ramp 1:2 °C/min; 270 °C 40 min; run time 130 min;  
 Detector: FID; heater = 300 °C; H<sub>2</sub> flow = 30 ml/min; air flow = 300 ml/min; make up flow = 40 ml/min.



$V_m$	155	[cm <sup>3</sup> (STP) g <sup>-1</sup> ]
$a_{s,BET}$	678	[m <sup>2</sup> g <sup>-1</sup> ]
C	102830	
Total pore volume( $p/p_0=0.990$ )	0.39	[cm <sup>3</sup> g <sup>-1</sup> ]
Average pore diameter	2.29	[nm]

**Fig. 7** BET plot of Pd-NP-AC catalyst

## Results and discussion

Pd-NP-AC was prepared by the method described by Mamlouk et al. [22] with some modifications. The structure of prepared compounds was characterized with various techniques, including TEM, BET, XRD and AAS. The XRD pattern of the Pd-NP-AC sample is shown in Fig. 2.

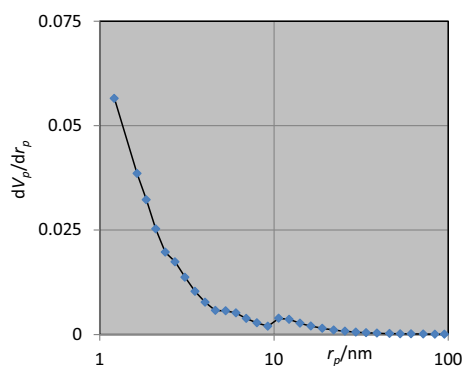


**Fig. 8** BJH plot of Pd-NP-AC catalyst

**Table 1** Comparison of different catalysts with our catalyst in the disproportionation of rosin

Catalyst	Wt% of catalyst	AA%	DAA%	Reaction time <sup>a</sup> (h)
Pd-NP-AC	0.05	0.07	70	3
FeCl <sub>3</sub>	1	35	19	2
FeCl <sub>3</sub> -I <sub>2</sub>	1	0.42	51	6
S-I <sub>2</sub>	1	2	72	6
S	1	56	24	2
KI	1	11	50	3
Fe-LiI	1	4.3	45	6
Fe-I <sub>3</sub>	1	22.44	30	5

<sup>a</sup> They are the time it takes to reach maximum conversion. All reactions were carried out at 280 °C

**Table 2** Recyclability test of Pd-NP-AC catalyst

DAA%	DAA%	DAA%
1st run	2nd run	3rd run
70	70	68

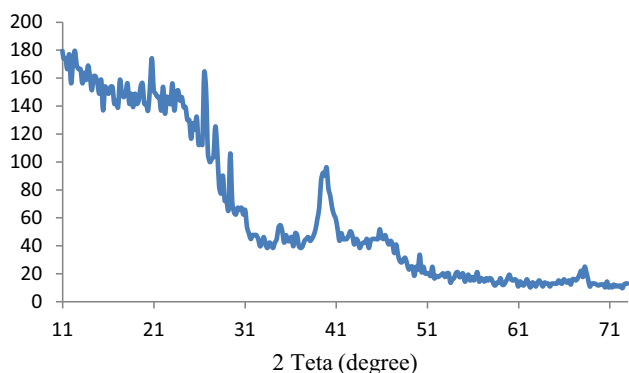


**Fig. 9** The XRD pattern of the recovered catalyst after the third run

In the spectra the sharp and narrow peaks at  $2\theta = 40^\circ$ ,  $46.6^\circ$ ,  $68^\circ$ ,  $82^\circ$  and  $87^\circ$ , which correspond to (111), (200), (220), (311) and (222) crystalline planes of Pd, were

attributed to the presence of crystalline palladium and indicating that palladium element exists in the form of Pd(0). All diffraction peaks and positions for palladium match well with those from the JCPDS card no. 05-0681. The crystallite size of palladium nanoparticles was evaluated using Scherrer equation for the (111) peak at  $2\theta = 40^\circ$  and was found to be 15 nm in size. The assignments are concordant with the Sarioglan [23], Drelinkiewicz et al. [24] and Zamani and Hossieni [25]. These crystalline palladium peaks were well separated from the broad peak of AC at around  $2\theta = 26^\circ$  which corresponds to the peak of graphite [26].

A TEM was used to obtain direct information about the structure and morphology of the palladium nanoparticles. Figure 3 shows the TEM images of the Pd-NP-AC. The mean diameter of palladium nanoparticles is about 10–45 nm with a mostly spherical shape.

Figure 4 shows the chemical maps of the Pd-NP-AC catalyst. It can be seen from the figure that the maps for palladium and carbon clearly reveal their presence in the structure of the catalyst. The amount of palladium (4.65%) of Pd-NP-AC was determined by atomic absorption analysis.

AC is a highly porous substance and has an extremely large surface area. The SEM of the Pd-NP-AC catalyst (Fig. 5) shows the porous characteristics of AC. To obtain detailed information about the pore volume, pore size distribution, and specific surface area, the N<sub>2</sub> adsorption and desorption isotherms at 77 K are performed on the samples (Fig. 6). BET indicated that surface area of the Pd-NP-AC is 678 m<sup>2</sup>/g while total pore volume is 0.39 cm<sup>3</sup>/g (Fig. 7). The average pore size diameter was calculated to be 2.29 nm using BJH methods (Fig. 8).

Disproportionation of rosin involves dehydrogenation, isomerisation and hydrogenation reactions of abietic-type acids so that the mixture of acids evolves to a final composition that is more stable from a thermodynamical viewpoint. The catalytic behavior of the Pd-NP-AC nanoparticles was studied for disproportionation of gum rosin and the progress of reaction was monitored by GC. In the GC spectrums, the peak at 98.6 min was from AA and the peak at 96.5 min was from DAA. The progress of reaction is monitored as an increase in DAA peak and decrease in AA peak. When the reaction was carried out with 0.1% (w/w) of catalyst at 280 °C for 5 h, DPR was obtained with a 72.4% yield. After evaluation of the catalytic efficiency, the optimization of time and temperature showed that the best result was obtained after 3 h at 280 °C using 0.05% (w/w) of catalyst in nitrogen. Under this condition, DPR was obtained with a 70% yield. A comparison with other reported efficient catalysts for the disproportionation of rosin demonstrated that our present catalytic

system exhibited a higher conversion and yield (see supplementary material) (Table 1).

An important issue related to solid catalysts is reusability. The reusability of the Pd-NP-AC catalyst was also studied. To recycle the catalyst, the catalyst was filtered from the reaction, washed with hot 2-propanol and dried for the next cycle at 80 °C. The Pd-NP-AC catalyst showed good stability for at least three runs in terms of DAA% (Table 2). The XRD pattern of the recovered catalyst after the 3rd run is shown in Fig. 9. In the spectra, the sharp and narrow peaks at  $2\theta = 40^\circ$ ,  $46.6^\circ$  and  $68^\circ$  were attributed to the presence of crystalline palladium [23–26].

## Conclusions

In this paper, the catalytic disproportionation of Gum rosin over palladium nanoparticles loaded on AC was investigated. The catalyst was characterized by TEM, XRD, BET and AAS. Compared with other reported efficient catalysts in the literature, Pd-NP-AC is among the best catalysts for the disproportionation of rosin.

**Acknowledgements** We acknowledge Tarbiat Modares University, Iran National Science Foundation (INSF) and Padideh Shimi Jam Co. for support of this work.

**Open Access** This article is distributed under the terms of the Creative Commons Attribution 4.0 International License (<http://creativecommons.org/licenses/by/4.0/>), which permits unrestricted use, distribution, and reproduction in any medium, provided you give appropriate credit to the original author(s) and the source, provide a link to the Creative Commons license, and indicate if changes were made.

## References

- Souto, J.C., Yustos, P., Ladero, M., Garcia-Ochoa, F.: Disproportionation of rosin on an industrial Pd/C catalyst: reaction pathway and kinetic model discrimination. *Bioresour. Technol.* **102**, 3504–3511 (2011)
- Wang, L., Chen, X., Sun, W., Liang, J., Xu, X., Tong, Z.: Kinetic model for the catalytic disproportionation of pine oleoresin over Pd/C catalyst. *Ind. Crop. Prod.* **49**, 1–9 (2013)
- Mayer, M.J.J., Meuldijk, J., Thoenes, D.: Influence of disproportionated rosin acid soap on the emulsion polymerization kinetics of styrene. *J. Appl. Polym. Sci.* **56**, 119–126 (1995)
- Gonzalez, M.A., Pérez-Guaita, D., Correa-Royero, J., Zapata, B., Agudelo, L., Mesa-Arango, A., Betancur-Galvis, L.: Synthesis and biological evaluation of dehydroabiatic acid derivatives. *Eur. J. Med. Chem.* **45**, 811–816 (2010)
- Tanaka, R., Tokuda, H., Ezaki, Y.: Cancer chemopreventive activity of rosin constituents of *Pinus spez.* and their derivatives in two-stage mouse skin carcinogenesis test. *Phytomedicine* **15**, 985–992 (2008)
- Fonseca, T., Gigante, B., Marques, M.M., Gilchrist, T.L., De Clercq, E.: Synthesis and antiviral evaluation of benzimidazoles, quinoxalines and indoles from dehydroabiatic acid. *Bioorg. Med. Chem.* **12**, 103–112 (2004)
- Häkkinen, S.T., Lackman, P., Nygrén, H., Oksman-Caldentey, K.M., Maaheimo, H., Rischer, H.: Differential patterns of dehydroabiatic acid biotransformation by *Nicotiana tabacum* and *Catharanthus roseus* cells. *J. Biotechnol.* **157**, 287–294 (2012)
- Brites, M.J., Guerreiro, A., Gigante, B., Marcelo-Curto, M.J.: Quantitative determination of dehydroabiatic acid methyl ester in disproportionated rosin. *J. Chromatogr.* **641**, 199–202 (1993)
- Pinghui, Z., Zhendong, Z., Liangwu, B., Yanju, L., Dongmei, L.: Review on colorless disproportionated rosin and its catalysts. *J. Bioprocess. Eng. Biorefin.* **1**, 140–147 (2012)
- Jadhav, J.: Process to Produce Disproportionate rosin Based Emulsifier for Emulsion Polymerization. US Patent 6087318 (2000)
- Zhao, G., Rouge, B.: Method of Producing Disproportionated Rosin. US Patent 0097061 A1 (2008)
- Song, Z.Q., Zavarin, E., Zinkel, D.F.: On the palladium-on-charcoal disproportionation of rosin. *J. Wood Chem. Technol.* **5**, 535–542 (1985)
- Fleck, E.E., Palkin, S.: Catalytic isomerization of the acids of pine oleoresin and rosin. *J. Am. Chem. Soc.* **59**, 1593–1595 (1937)
- Fleck, E.E., Palkin, S.: On the nature of pyroabiatic acids. *J. Am. Chem. Soc.* **60**, 921–925 (1938)
- Enos, H.I., Harris, G.C., Hedrich, G.W.: Rosin and rosin derivatives. In: Mark, H.F., McKetta Jr., J.J., Othmer, D.F. (eds.) *Kirk–Othmer Encyclopedia of Chemical Technology*, vol. 17, 2nd edn, p. 475. Wiley, New York (1968)
- Mostafalu, R., Banaei, A., Riazi, M.H., Ghorbani, F.: A modified method for the determination of *N*-nitrosodiethanolamine in coconut diethanolamide using HPLC with dual-wavelength UV–Vis detector. *J. Surfactants Deterg.* **19**, 431–435 (2016)
- Mostafalu, R., Banaei, A., Ghorbani, F.: An inaccuracy in the determination of cocoamidopropyl betaine by the potentiometric method. *J. Surfactants Deterg.* **18**, 919–922 (2015)
- Kaboudin, B., Mostafalu, R., Yokomatsu, T.: Fe<sub>3</sub>O<sub>4</sub> nanoparticle-supported Cu(II)- $\beta$ -cyclodextrin complex as a magnetically recoverable and reusable catalyst for the synthesis of symmetrical biaryls and 1,2,3-triazoles from aryl boronic acids. *Green Chem.* **15**, 2266–2274 (2014)
- Mostafalu, R., Kaboudin, B., Kazemi, F., Yokomatsu, T.: *N*-arylation of amines: C–N coupling of amines with arylboronic acids using Fe<sub>3</sub>O<sub>4</sub> magnetic nanoparticles-supported EDTA–Cu(II) complex in water. *RSC Adv.* **4**, 49273–49279 (2014)
- Arefi, M., Heydari, A.: Transamidation of primary carboxamides, phthalimide, urea and thiourea with amines using Fe(OH)<sub>3</sub>@-Fe<sub>3</sub>O<sub>4</sub> magnetic nanoparticles as an efficient recyclable catalyst. *RSC Adv.* **6**, 24684–24689 (2016)
- Arefi, M., Saberi, D., Karimi, M., Heydari, A.: Superparamagnetic Fe(OH)<sub>3</sub>@Fe<sub>3</sub>O<sub>4</sub> nanoparticles: an efficient and recoverable catalyst for tandem oxidative amidation of alcohols with amine hydrochloride salts. *ACS Comb. Sci.* **17**, 341–347 (2015)
- Alvarez, G.F., Mamlouk, M., Senthil-Kumar, S.M., Scott, K.: Preparation and characterization of carbon-supported palladium nanoparticles for oxygen reduction in low temperature PEM fuel cells. *J. Appl. Electrochem.* **41**, 925–937 (2011)
- Sarioglan, S.: Recovery of palladium from spent activated carbon-supported palladium catalysts. *Platin. Met. Rev.* **57**, 289–296 (2013)
- Drelinkiewicz, A., Hasik, M., Kloc, M.: Pd/polyaniline as the catalysts for 2-ethylanthraquinone hydrogenation. The effect of palladium dispersion. *Catal. Lett.* **64**, 41–47 (2000)



25. Zamani, F., Hosseini, S.M.: Palladium nanoparticles supported on  $\text{Fe}_3\text{O}_4$ /amino acid nanocomposite: highly active magnetic catalyst for solvent-free aerobic oxidation of alcohols. *Catal. Commun.* **43**, 164–168 (2014)
26. Gupta, A.K., Ganeshan, K., Sekhar, K.: Adsorptive removal of water poisons from contaminated water by adsorbents. *J. Hazard. Mater.* **137**, 396–400 (2006)

